Supporting Information

Enhanced Ion Conductivity through Hydrated, Polyelectrolyte-grafted Cellulose Nanocrystal Films

James H. Lettow[1], Richard Y. Kaplan[1], Paul F. Nealey[1], Stuart J. Rowan[1,2,3*]*

[1] Pritzker School of Molecular Engineering, University of Chicago, 5640 S. Ellis Ave., Chicago, IL 60637, USA

[2] Department of Chemistry, University of Chicago, 5735 S Ellis Ave., Chicago, IL 60637, United States

[3] Chemical and Engineering Sciences Division, Argonne National Laboratory, 9700 Cass Avenue, Lemont, Illinois 60439, United States

[*]**E-mail:** nealey@uchicago.edu, stuartrowan@uchicago.edu

TABLE OF CONTENTS

POLY(2-VINYLPYRIDINE) CHARACTERIZATION

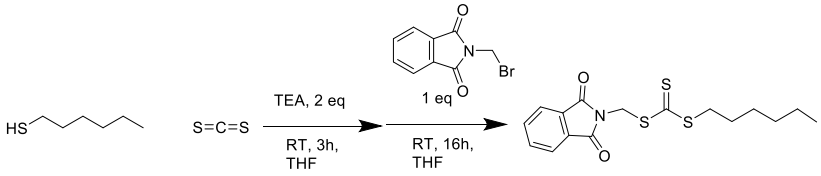

Scheme S1: Synthesis of the chain transfer agent phthalimidomethyl hexyl trithiocarbonate

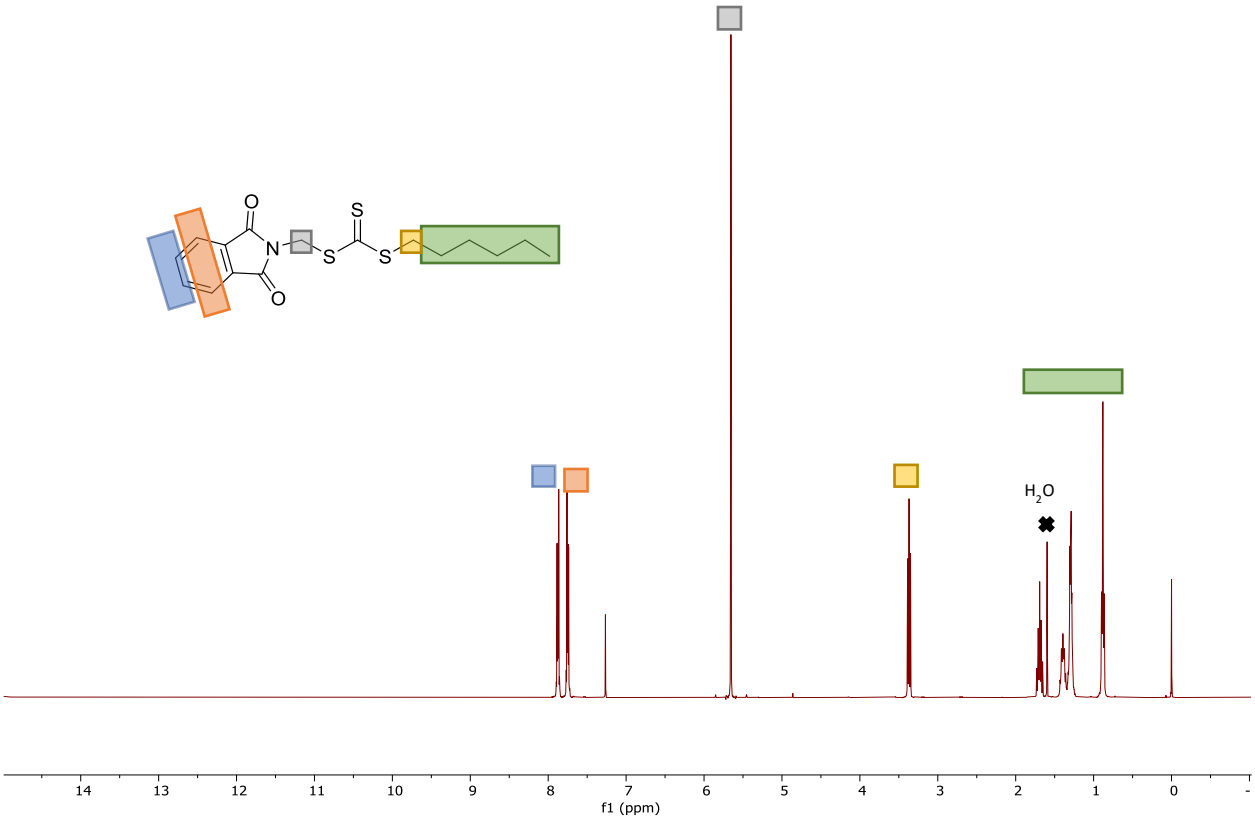

Figure S1: ^{1}H NMR (500 MHz, $CDCl_3$) spectra of phthalimidomethyl hexyl trithiocarbonate

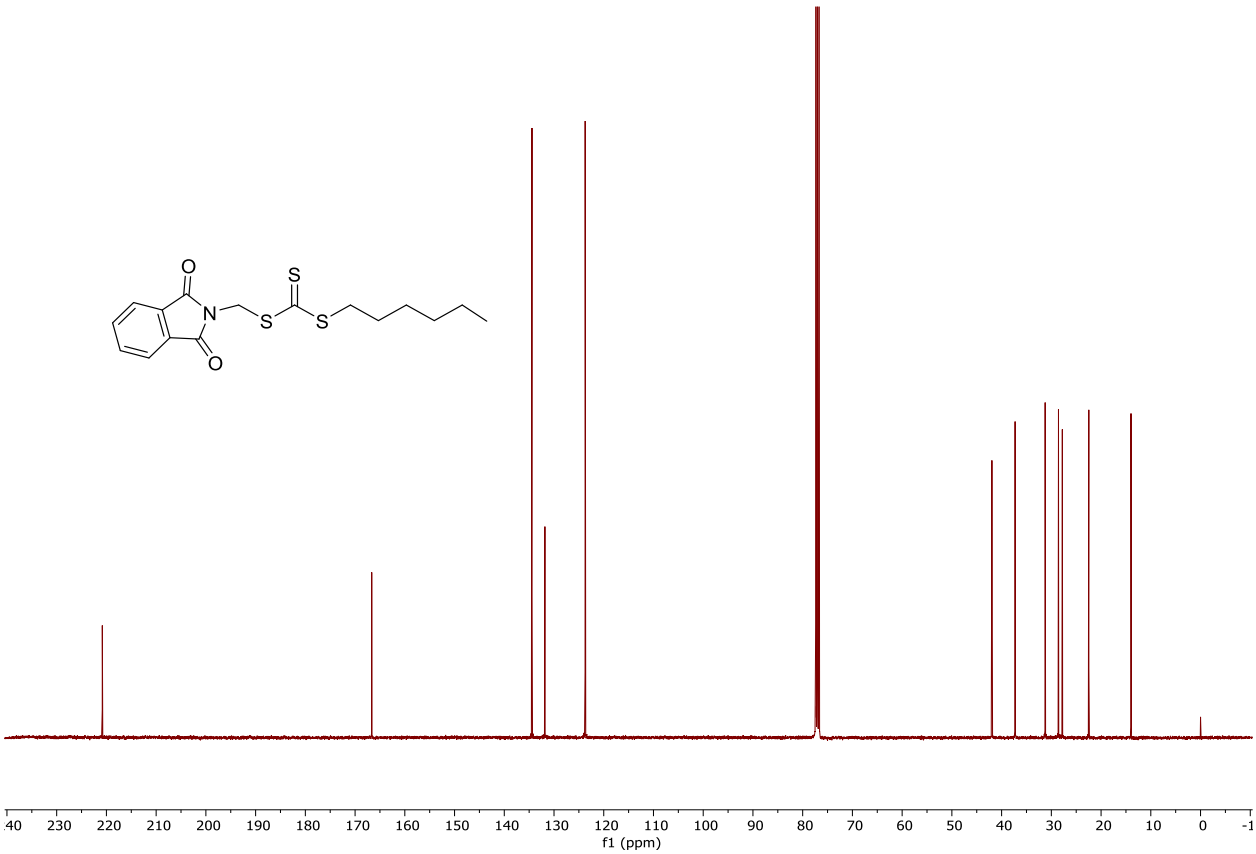

Figure S2: ^{13}C NMR (101 MHz, $CDCl_3$) spectra of phthalimidomethyl hexyl trithiocarbonate

Table S1: Homopolymer Synthesis Summary

	M_n, ^1H NMR (g/mol)	M_n, GPC-MALS (g/mol)	Degree of Polymerization (DP)	Dispersity, $Đ$
PV-SH$_{68}$	6900	7100	68	1.14
PV-SH$_{113}$	11100	11900	113	1.20
PV-SH$_{150}$	15700	15800	150	1.24
PV-SH$_{286}$	29400	30000	286	1.17
PS$_{324}$	34100	34200	329	1.02

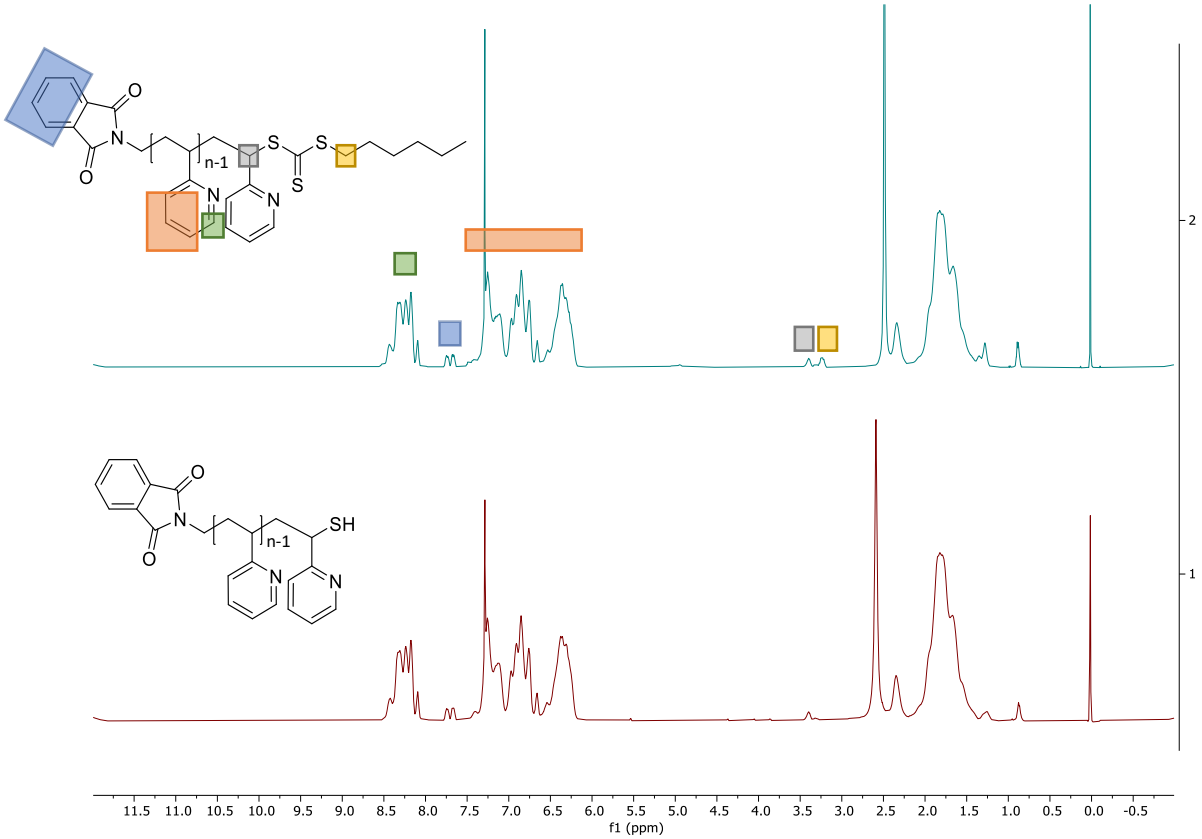

Figure S3: ^{1}H NMR (500 MHz, $CDCl_3$) spectra of **PV_{68}** (top, teal) and **PV-SH_{68}** (bottom, red) which shows the diminishment of the 3.3 ppm peak indicative of trithiocarbonate to thiol conversion

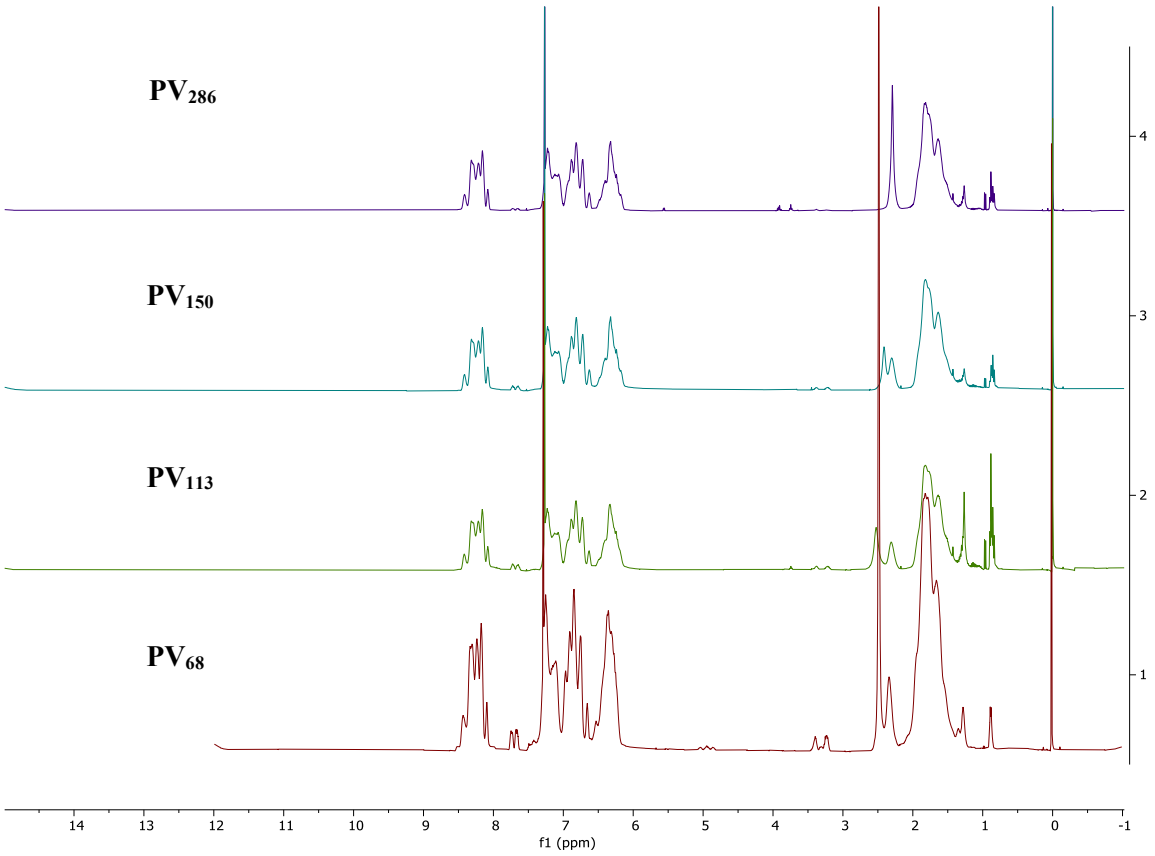

Figure S4: ^{1}H NMR (500 MHz, $CDCl_3$) spectra of **PV_{68}, PV_{113}, PV_{150},** and **PV_{286}** which permit analysis of molecular weight by end group analysis

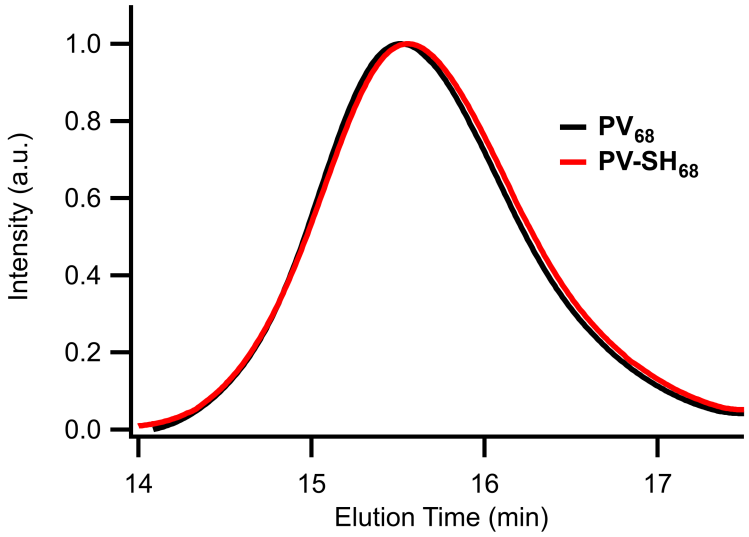

Figure S5: GPC-MALS of **PV_{68}** (black) and **PV-SH_{68}** (red).

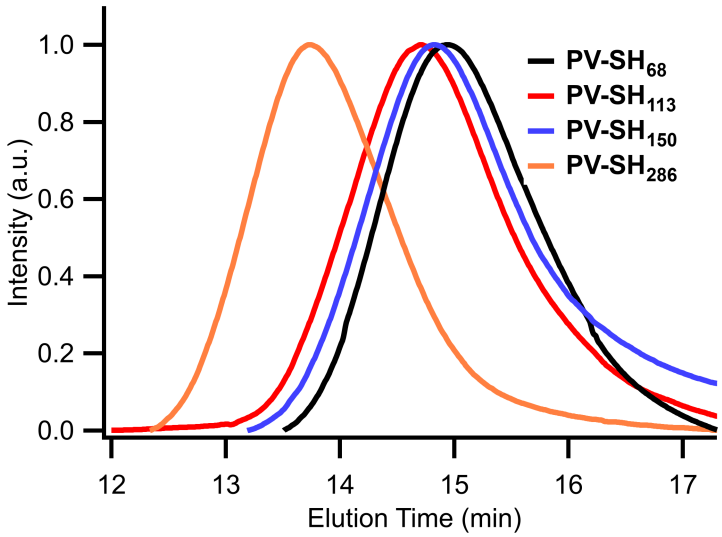

Figure S6: GPC-MALS **PV-SH$_{68}$, PV-SH$_{113}$, PV-SH$_{150}$,** and **PV-SH$_{286}$.**

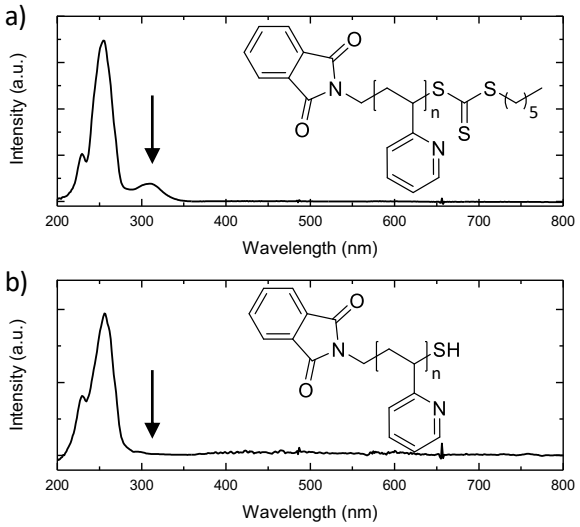

Figure S7: UV-Vis of a) **PV$_{68}$** and b) **PV-SH$_{68}$** with demarcation of the diminution of the 310 nm peak

Table S2: Diblock copolymer synthesis summary with regard to each block

	M_n, 1, ^{1}H NMR (g/mol)	M_n, 1, GPC-MALS (g/mol)	M_n, 2, GPC-MALS (g/mol)	f_{PV}	M_n Total (g/mol)	Dispersity, $Đ$
PV-PS-SH$_{286,150}$	29400	30000	15600	0.65	45600	1.17
PS-PV-SH$_{329,86}$	34100	34200	9000	0.21	43200	1.13

CELLULOSE NANOCRYSTAL CHARACTERIZATION

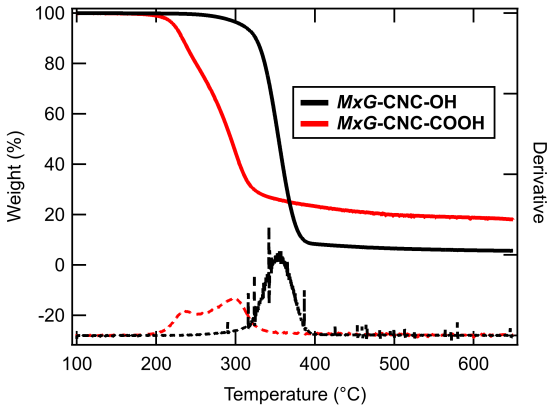

Figure S8: Thermal Gravimetric Analysis (TGA) of ***MxG*-CNC** before and after TEMPO oxidation (under nitrogen atmosphere with a heating rate of 10 °C/min).

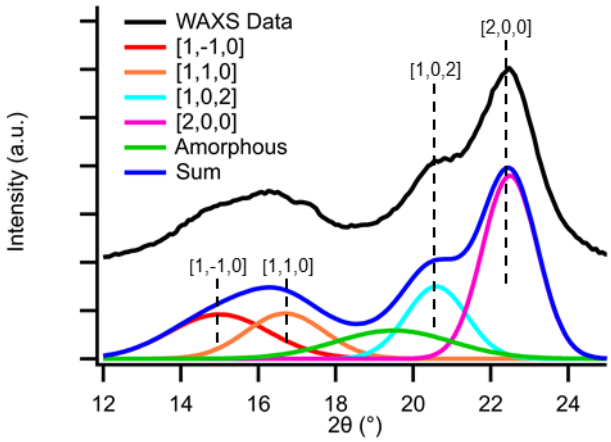

Figure S9: WAXS of ***MxG*-CNC-COOH** with labeled crystalline peaks and Gaussian fit to calculate crystallinity index. The Gaussian peaks corresponding to the various CNC crystal planes are notated by color. Note that original WAXS data is offset for clarity.

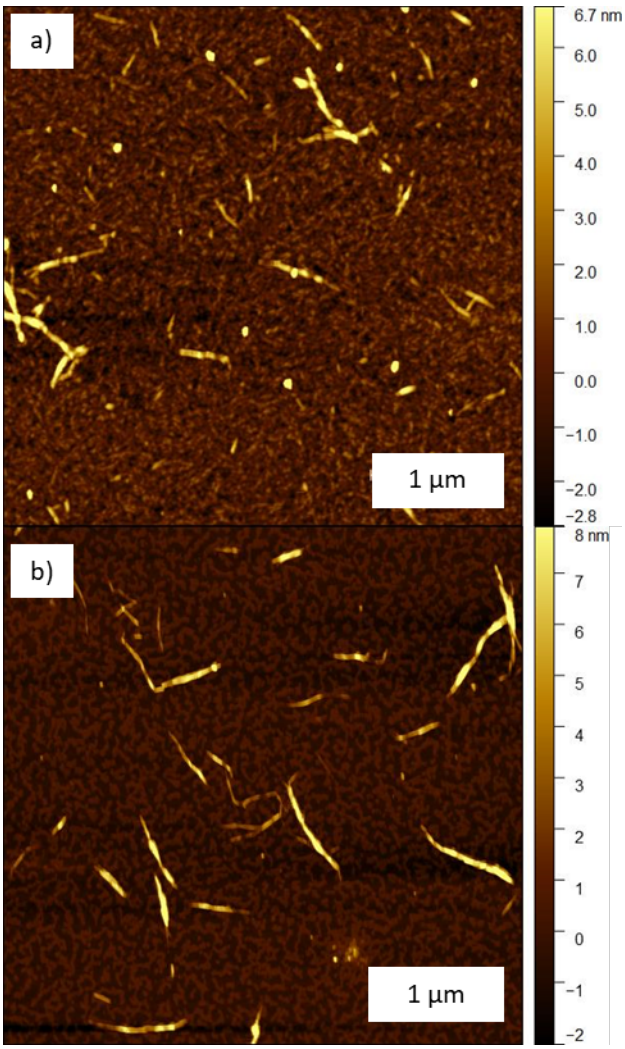

Figure S10: AFM height images of a) ***MxG*-CNC-COOH** and b) ***MxG*-CNC-Allyl** cast on poly-L-lysine coated mica

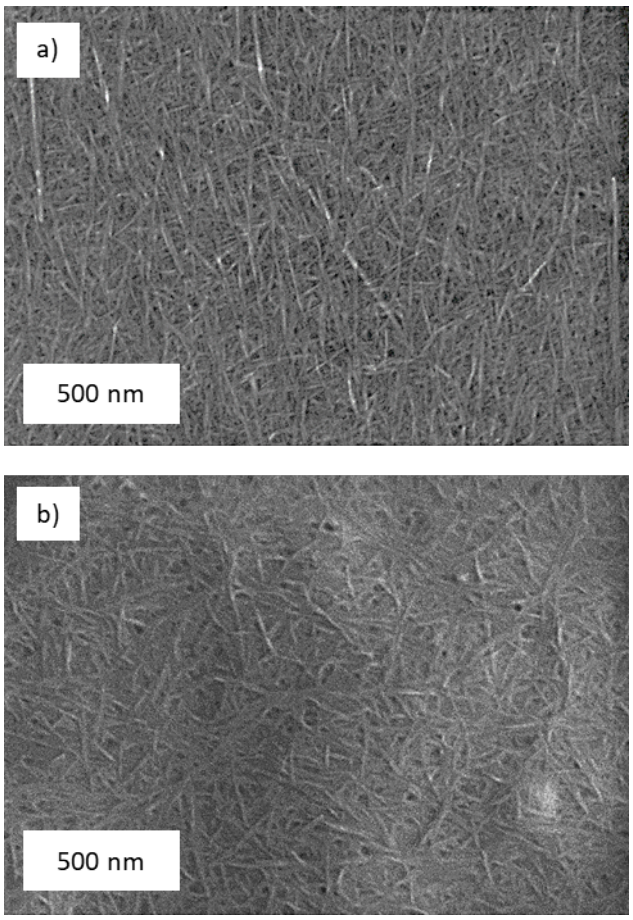

Figure S11: SEM of a) ***MxG*-CNC-COOH** and b) ***MxG*-CNC-Allyl** as cast from solvent exchanged solution and coated in 2 nm Pt/Pd

POLYMER GRAFTED NANOPARTICLE CHARACTERIZATION

To calculate the volume fraction of polyelectrolyte ($VolFrac_{PE}$) in the ***MxG*-CNC-*g*-mPV** system, the following equation is used in accordance with literature precedent,[1]

$$VolFrac_{PE} = \frac{\frac{\Phi_{polymer}}{\rho_{polymer}} f_{P2VP} + \frac{\Phi_{polymer}}{MW_{2VP}} \frac{x_M MW_I}{\rho_I} f_{PV}}{\frac{\Phi_{polymer}}{\rho_{polymer}} + \frac{\Phi_{polymer}}{MW_{2VP}} \frac{x_M MW_I}{\rho_I} f_{PV} + \frac{\Phi_{CNC}}{\rho_{CNC}}} \quad \text{S1}$$

where Φ_{poly} and Φ_{CNC} are the weight fractions of polymer and CNC, respectively, $\rho_{polymer}$, ρ_I, and ρ_{CNC} are the densities of the polymer, iodomethane, and CNC, respectively, MW_{2VP} and MW_I are the molecular weights of 2-vinylpyridine and iodomethane, f_{PV} is the weight fraction of PV in a grafted PS-PV diblock copolymer and $x_M$is the methylation percentage of the polymer (65% in all cases). In this work, $\Phi_{polymer}$and Φ_{CNC} are determined by thermogravimetric analysis while $MW_{polymer}$ is determined by gel permeation chromatography, multiangle light scattering. Literature values of 1.5 g/cm^3 and 1.08 g/cm^3 was used for ρ_{CNC} and $\rho_{polymer}$ for PV and diblock copolymers, respectively.[2,3] For the case of grafted diblock copolymers, the individual block wt% must also be taken into account.

The surface density of allyl groups (σ_{allyl}), as number of allyl groups per nm^2, is given by,

$$\sigma_{allyl} = \frac{n_{allyl}}{SA_{CNC}} = \frac{\varphi_{allyl}\rho_{CNC}V_{CNC}N_A}{SA_{CNC}} \quad \text{S2}$$

where n_{allyl} is the number of allyl sites per CNC, φ_{allyl} is the density of allyl groups given as mmol/kg, ρ_{CNC} is the CNC density, V_{CNC} is the volume of an individual CNC, and SA_{CNC} is the surface area of an individual CNC. For determining φ_{allyl}, the difference was taken of sample conductometric titration before adding allylamine (1000 mmol/kg) and after (400 mmol/kg) resulting in a value of 600 mmol of allyl groups per kg of CNC. Literature values of 1.5 g/cm^3 was used for ρ_{CNC}.[2] V_{CNC} and SA_{CNC} are both calculated using literature values for *MxG*-CNC, a rectangular prism with dimensions 8.5nm by 2.8nm by 300nm as determined by SANS.[4] The value of σ_{allyl} is calculated to be 0.55 allyl groups per nm^2.

To calculate the polymer grafting density on CNC, $\sigma_{polymer}$, the density of polymer chains ($\varphi_{polymer}$) as given as mmol/kg can be defined as

$$\varphi_{polymer} = \frac{\Phi_{polymer}}{\Phi_{CNC}MW_{polymer}} \quad \text{S3}$$

where $\Phi_{polymer}$ is the weight fraction polymer, Φ_{CNC} is the weight fraction CNC, and $MW_{polymer}$ is the polymer molecular weight. By performing a similar analysis to equation S2 and inserting equation S3, the polymer grafting density on CNC can be defined as

$$\sigma_{polymer} = \frac{\Phi_{polymer}\rho_{CNC}V_{CNC}N_A}{\Phi_{CNC}MW_{polymer}SA_{CNC}} \quad \text{S4}$$

where all of the input quantities are either literature values or measured quantities. The conversion of allyl sites to polymer grafted sites, x, can be defined as,

$$x = \frac{\sigma_{polymer}}{\sigma_{allyl}} = \frac{\Phi_{Poly}}{\Phi_{CNC}\varphi_{Allyl}MW_{polymer}} \quad \text{S5}$$

and has calculated values ranging from 4% to 21% depending on molecular weight of grafting polymer and number of times of re-reaction.

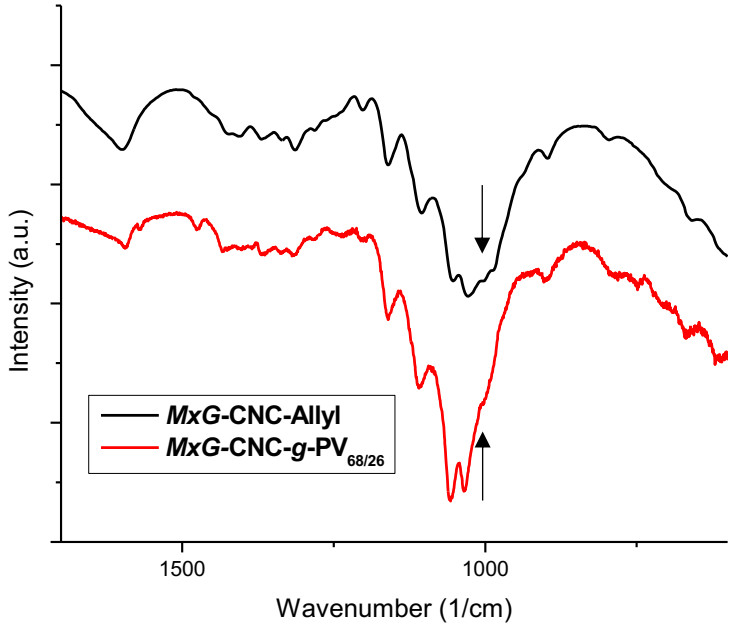

Figure S12: ATR-FTIR of ***MxG*-CNC-Allyl** and ***MxG*-CNC-*g*-PV$_{68/26}$**, with arrows highlighting the reduction of the C=C-H bend shoulder ca. 960-1010 cm^{-1}.

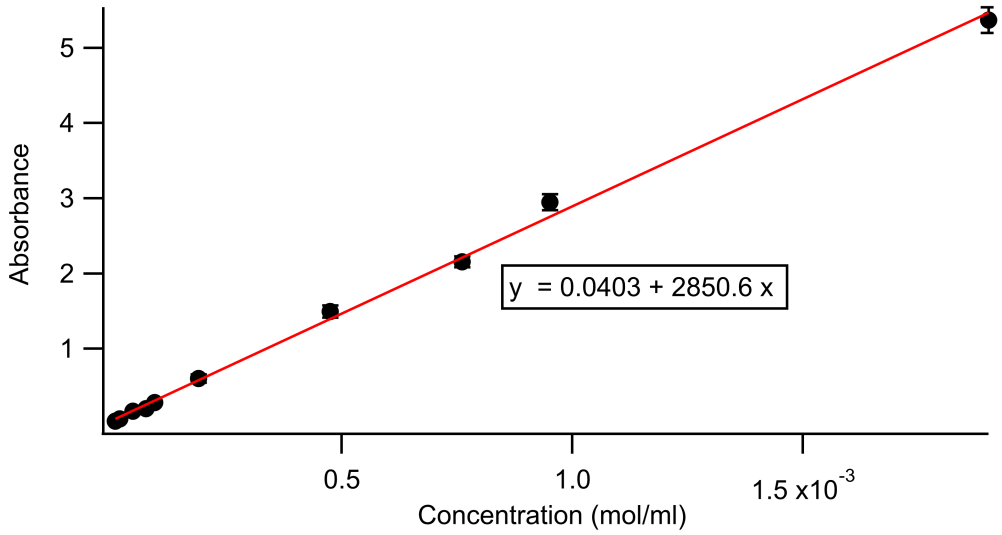

Figure S13: UV-Vis derived concentration data of **PV-SH$_{286}$** in methanol

Table S3: Concentration data and percentages of free polymer for given numbers of centrifugations of ***MxG*-CNC-*g*-mPV$_{286/62}$**

# of centrifuges	Concentration (mol/ml)	Polymer Removed (mg)	Free Polymer %
1	44.7	1650	827%
2	1.79	64.6	32%
3	0.441	15.9	8%
4	0.373	4.47	2%

Table S4: Summary of all PGN samples

Sample	Molecular Weight, M_n (g/mol) of polymer graft	Wt% Polymer	Vol% Polymer	Vol% Polymer when methylated	Grafting Density (chains/nm^2)
***MxG*-CNC-*g*-mPV$_{68/33}$**	7100	20%	26%	33%	0.03
***MxG*-CNC-*g*-mPV$_{68/57}$**	7100	40%	48%	57%	0.09
***MxG*-CNC-*g*-mPV$_{68/59}$**	7100	42%	50%	59%	0.10
***MxG*-CNC-*g*-mPV$_{68/64}$**	7100	47%	55%	64%	0.12
***MxG*-CNC-*g*-mPV$_{113/57}$**	11900	40%	48%	57%	0.05
***MxG*-CNC-*g*-mPV$_{113/62}$**	11900	45%	53%	62%	0.06
***MxG*-CNC-*g*-mPV$_{150/57}$**	15800	40%	48%	57%	0.04
***MxG*-CNC-*g*-mPV$_{150/66}$**	15800	50%	58%	66%	0.06
***MxG*-CNC-*g*-mPV$_{286/62}$**	30000	45%	53%	62%	0.03
***MxG*-CNC-*g*-mPV$_{286/82}$**	30000	70%	76%	82%	0.07
***MxG*-CNC-*g*-PS-mPV$_{150,286/60}$**	45600	50%	58%	60%	0.02
***MxG*-CNC-*g*-mPV-PS$_{86,329/64}$**	43200	50%	58%	64%	0.02

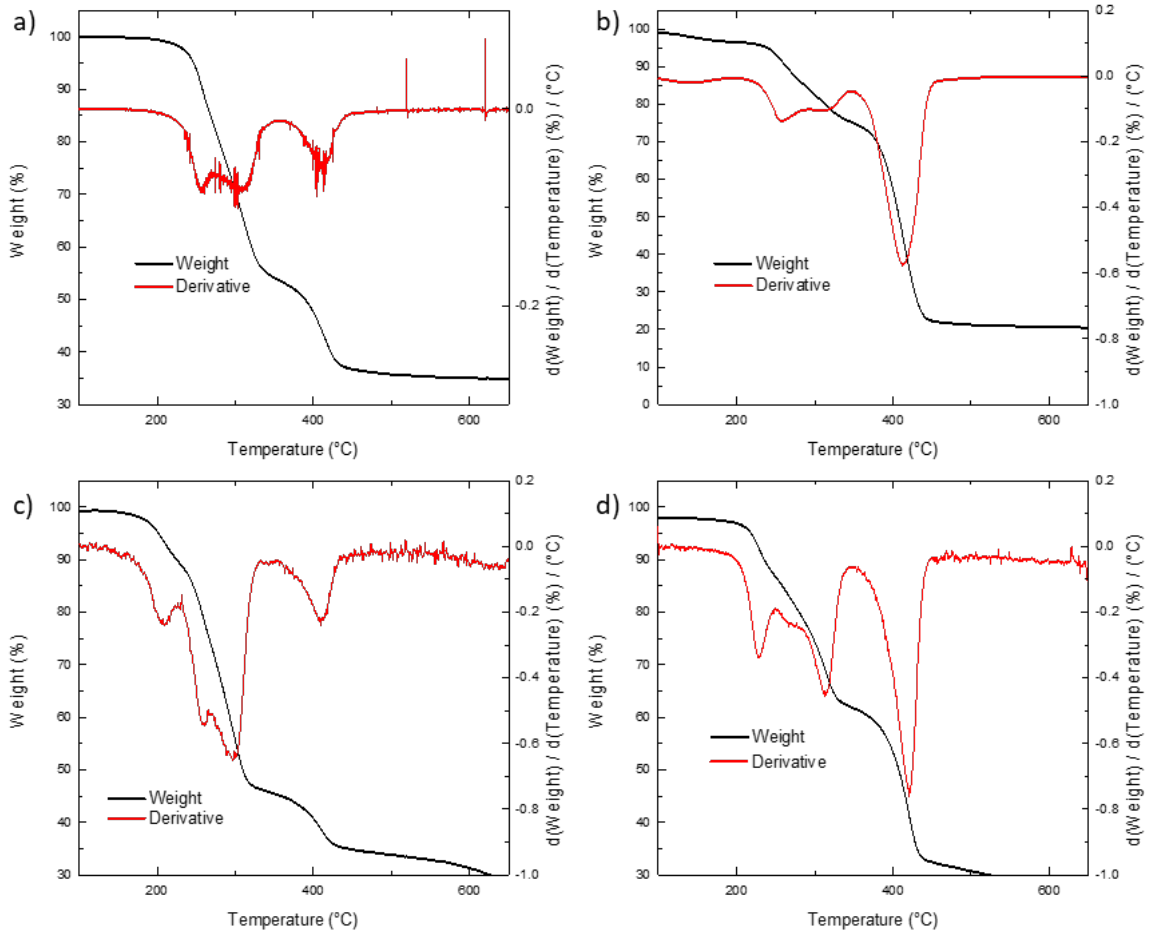

Figure S14: Thermogravimetric analysis (TGA) of ***MxG*-CNC-*g*-mPV$_{68/33}$** and ***MxG*-CNC-*g*-mPV$_{286/82}$** before (a, b) and after (c, d) methylation under nitrogen atmosphere with a heating rate of 10 °C/min.

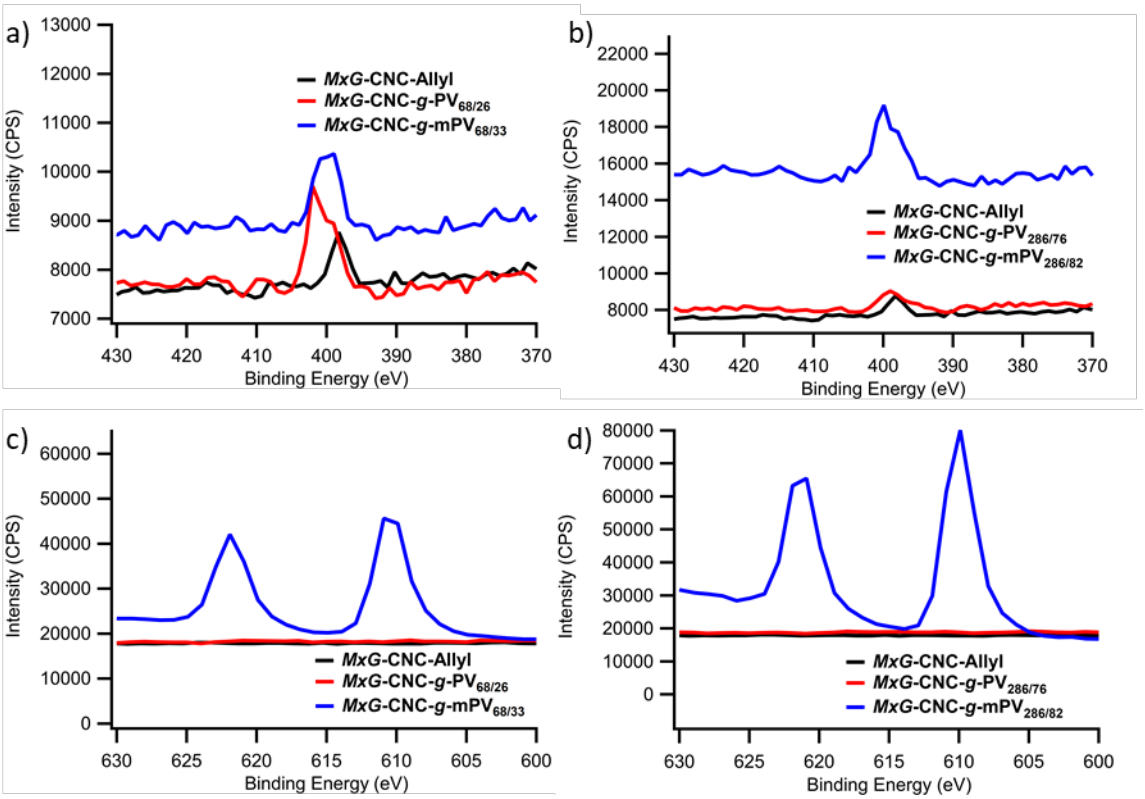

Figure S15: X-ray photoelectron spectroscopy (XPS) of nitrogen 1S peak comparing ***MxG*-CNC-Allyl** and both methylated and unmethylated a) ***MxG*-CNC-*g*-mPV$_{68/33}$** and b) ***MxG*-CNC-*g*-mPV$_{286/82}$** and the iodide 3D peaks comparing ***MxG*-CNC-Allyl** and both methylated and unmethylated c) ***MxG*-CNC-*g*-mPV$_{68/33}$** and d) ***MxG*-CNC-*g*-mPV$_{286/82}$.**

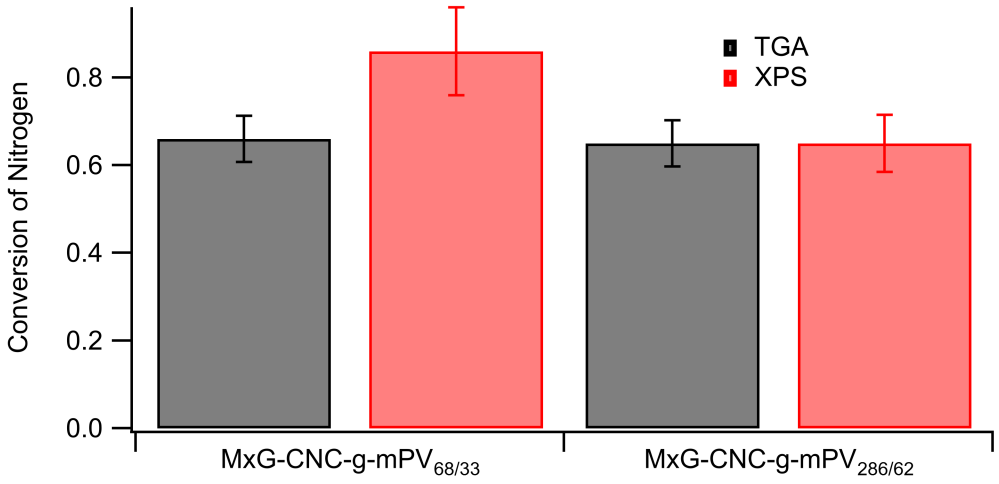

Figure S16: Measured degree of methylation of ***MxG*-CNC-*g*-mPV$_{68/33}$** and ***MxG*-CNC-*g*-mPV$_{286/82}$** obtained from TGA and XPS data.

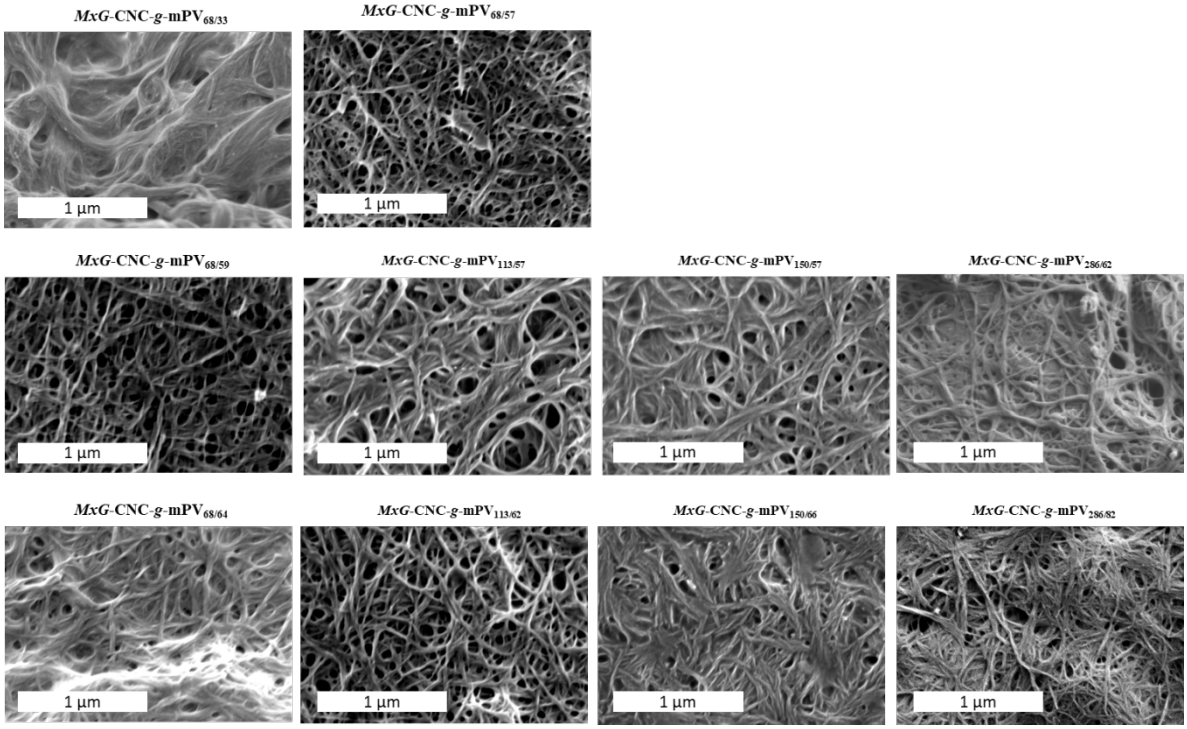

Figure S17: SEM of various ***MxG*-CNC-*g*-mPV**, as labeled coated in 2 nm Pt/Pd

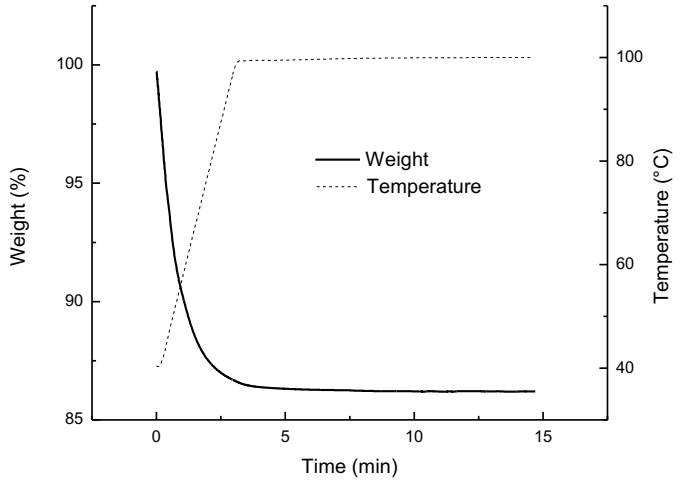

Figure S18: Characteristic TGA for measuring the water uptake of ***MxG*-CNC-*g*-mPV$_{286/82}$** at 95% RH

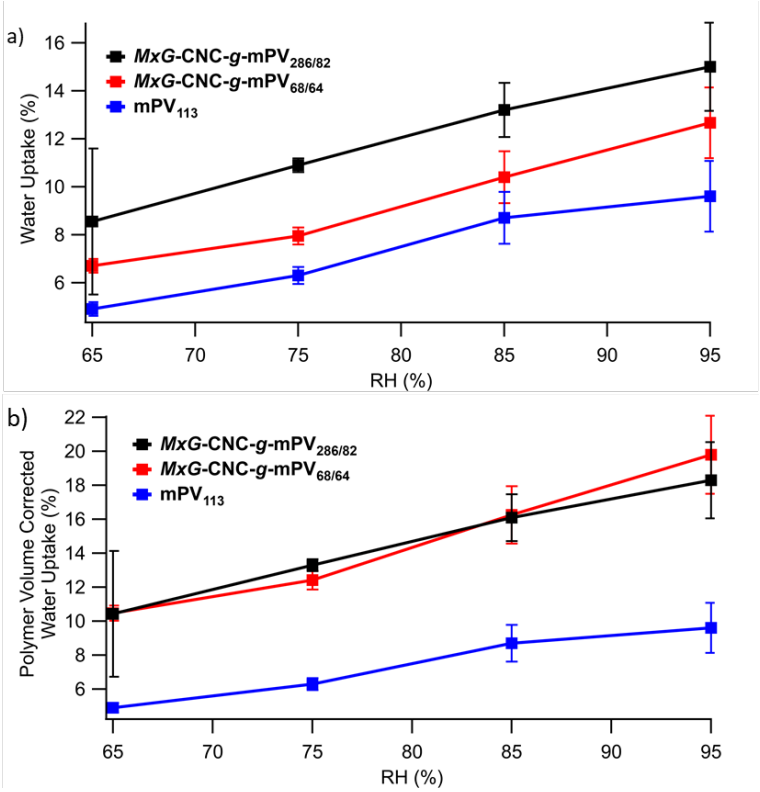

Figure S19: a) Measured water uptake and b) calculated water uptake of mPV component (adjusted for volume fraction of CNC) for ***MxG*-CNC-*g*-mPV$_{68/64}$** and ***MxG*-CNC-*g*-mPV$_{286/82}$**

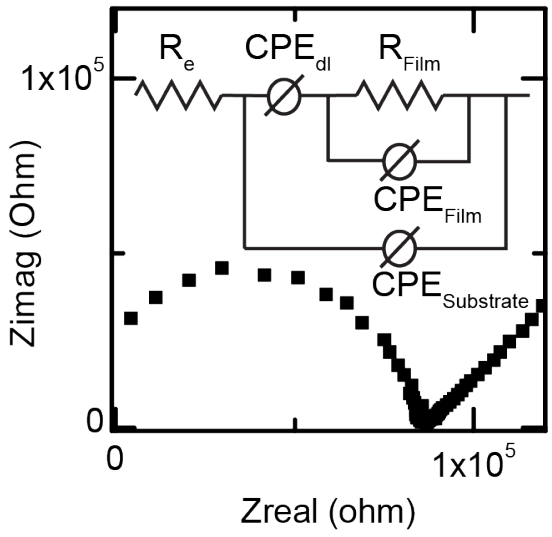

Figure S20: Nyquist plot and model fit for in-plane ***MxG*-CNC-*g*-mPV$_{68/33}$**

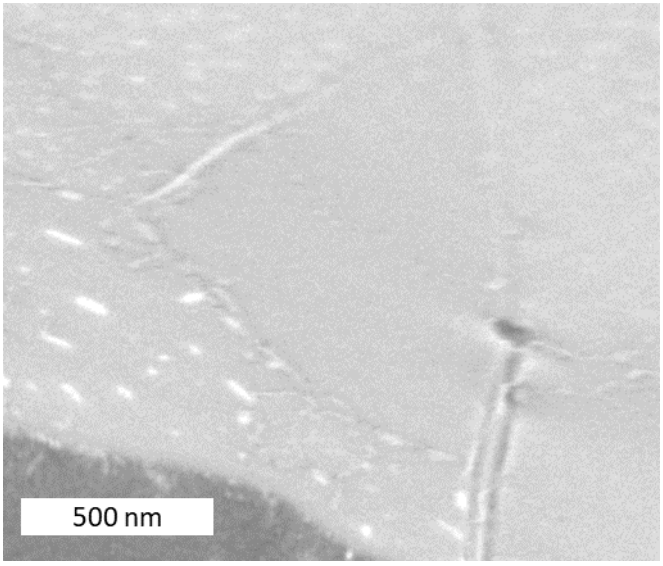

Figure S21: SEM of **mPV$_{68}$** with 10 vol% ***MxG*-CNC-Allyl** noting a flat surface in comparison to the individualized nanofibers of **Figure S16**.

DIBLOCK COPOLYMER SYNTHESIS AND CHARACTERIZATION

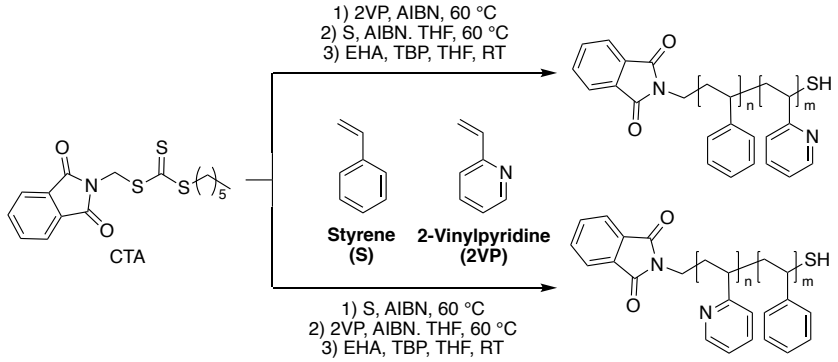

Scheme S2: Synthesis of the thiol-endcapped PS-PV block copolymers

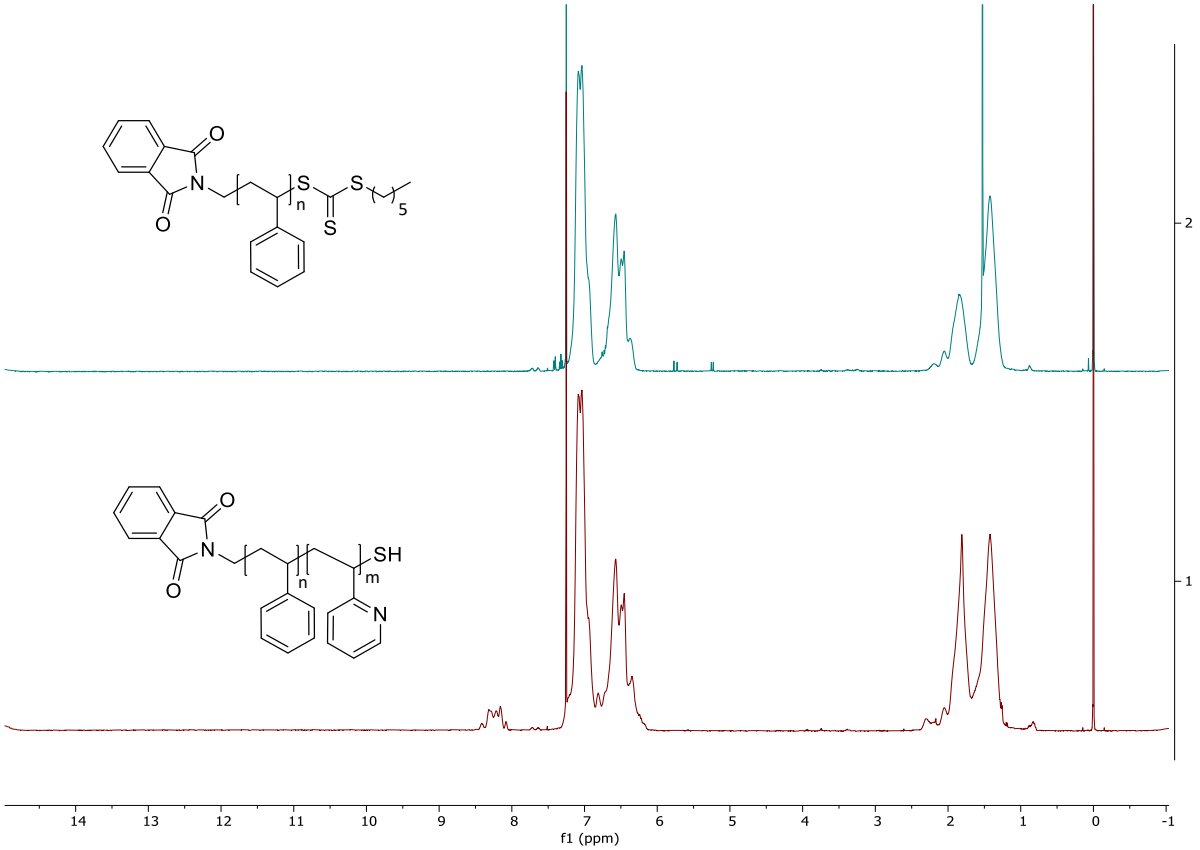

Figure S22: ^{1}H NMR (500 MHz, $CDCl_3$) spectra of **PS$_{329}$** and **PS-PV-SH$_{329,86}$**. Integration yields a f_{PV} = 0.21.

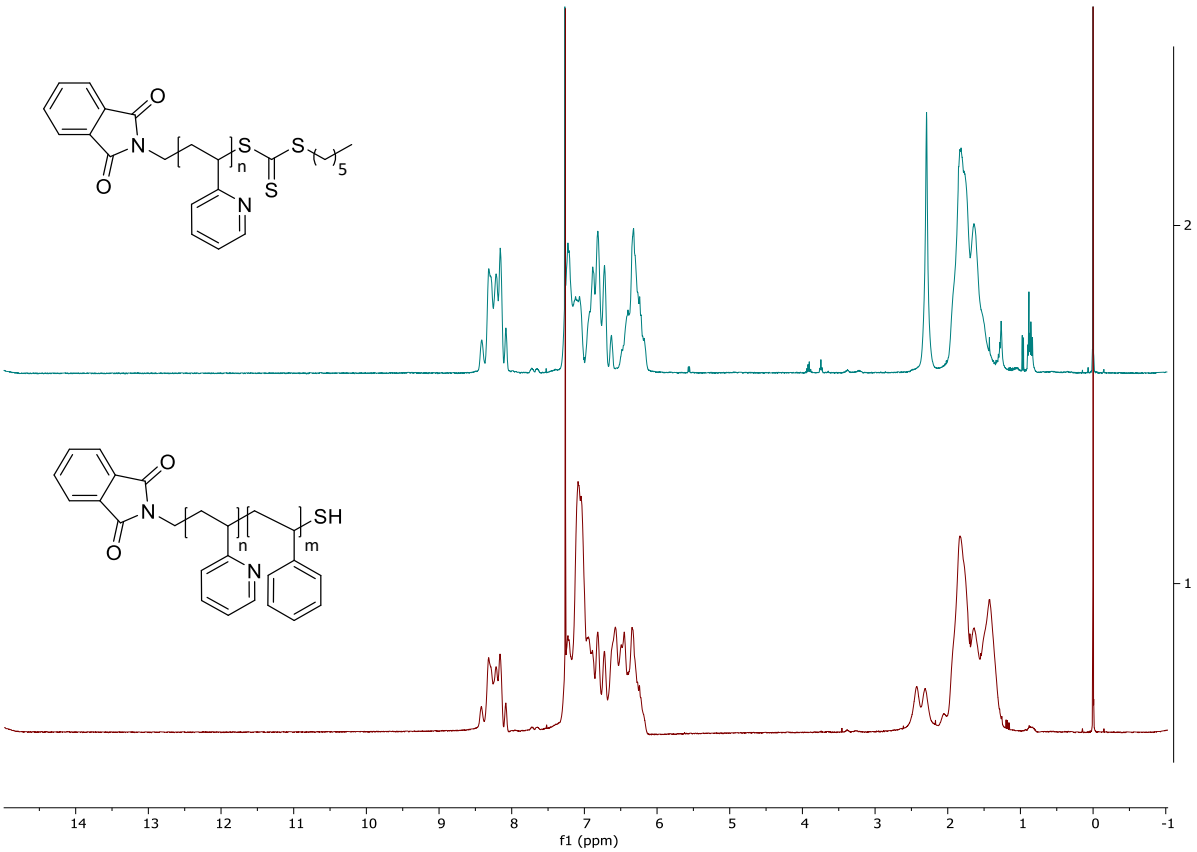

Figure S23: ^{1}H NMR (500 MHz, $CDCl_3$) spectra of **PV$_{286}$** and **PV-PS-SH$_{286,150}$**. Integration yields a f_{PV} = 0.65.

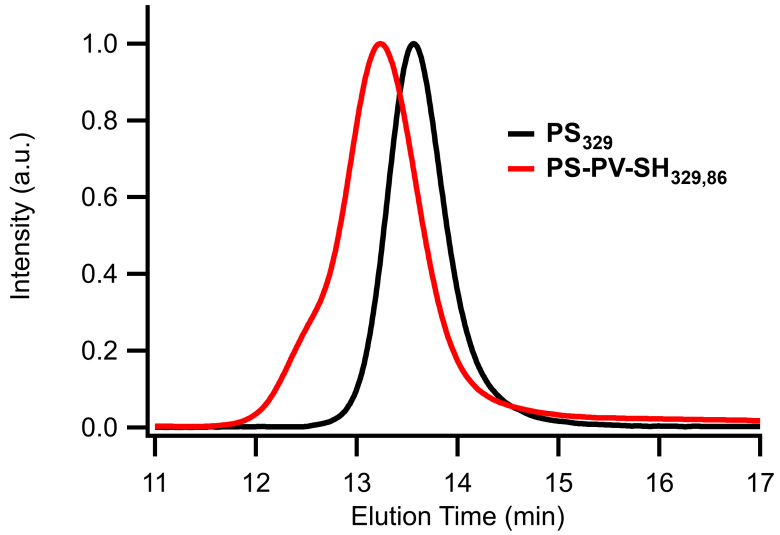

Figure S24: **PS-PV-SH$_{329,86}$** (red) and **PS$_{329}$** (black) GPC-MALS traces. Some chain end coupling is noted.

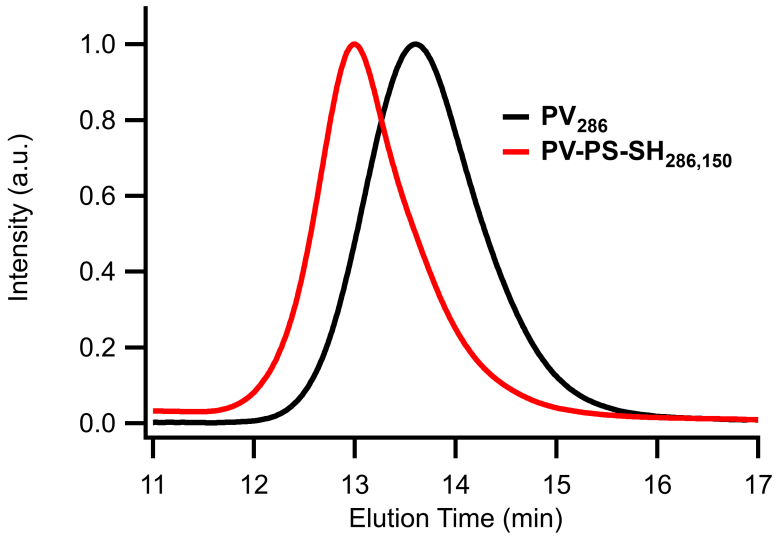

Figure S25: PV-PS-SH$_{286,150}$ (red) and **PV$_{286}$** (black) GPC-MALS Traces

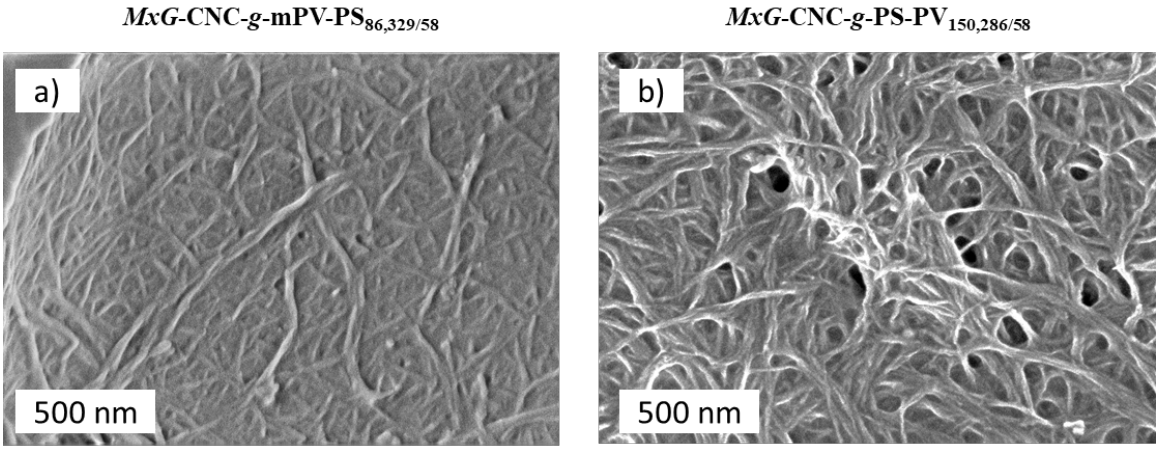

Figure S26: SEM of a) ***MxG*-CNC-*g*-PV-PS$_{86,329/58}$** and b) ***MxG*-CNC-*g*-PS-PV$_{150,286/58}$** coated in 2 nm Pt/Pd.

MEASURED EIS CHARACTERIZATION

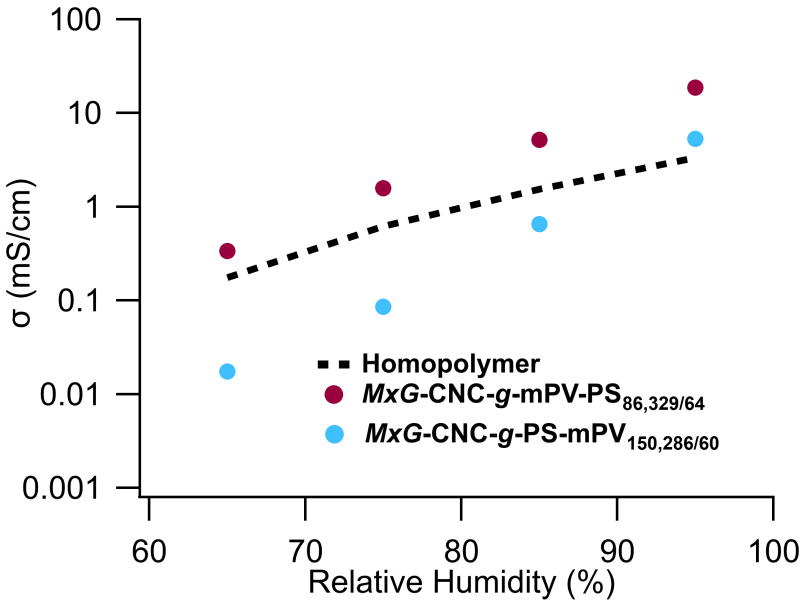

Figure S27: Measured conductivity data of the two diblock-grafted samples plotted against relative humidity along with **mPV** homopolymer (measured by IDE) for comparison (data adjusted for mPV volume fraction is shown in **Figure 4b**).

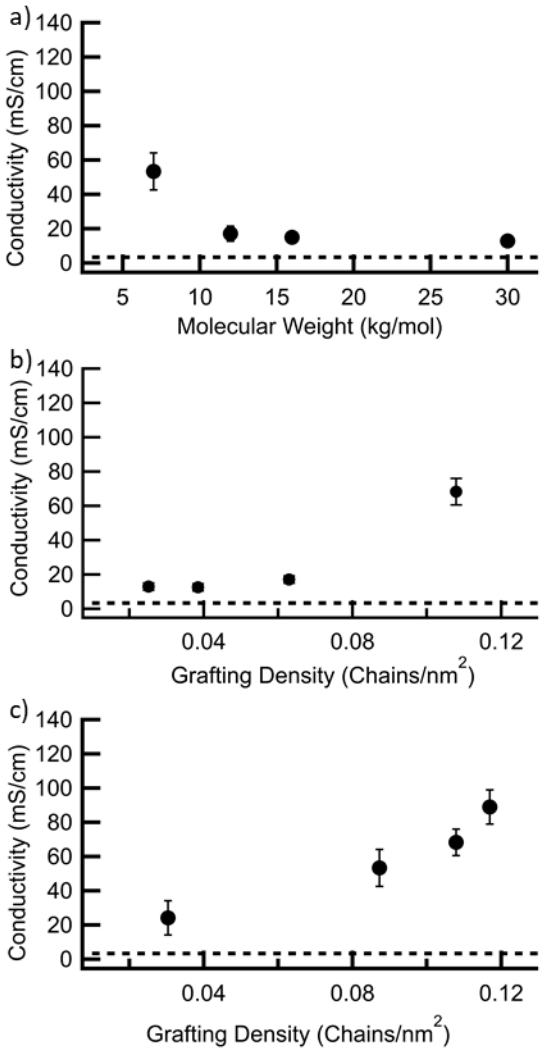

Figure S28: Measured conductivities of the **mPV** in the methylated PEGN films with a) similar grafting density but different molecular weight and grafting density, b) same volume fraction but differing molecular weights and grafting density, and c) same molecular weight grafted polyelectrolyte but different grafting density and volume fraction. Dotted lines correspond to conductivity of methylated homopolymer and all conductivity data is obtained from 95% relative humidity and room temperature samples. (data adjusted for **mPV** volume fraction is shown in **Figure 5**).

References

(1) Sharon, D.; Bennington, P.; Dolejsi, M.; Webb, M. A.; Dong, B. X.; De Pablo, J. J.; Nealey, P. F.; Patel, S. N. Intrinsic Ion Transport Properties of Block Copolymer Electrolytes. *ACS Nano* **2020**, *14* (7), 8902–8914. https://doi.org/10.1021/acsnano.0c03713.

(2) Eichhorn, S. J.; Dufresne, A.; Aranguren, M.; Marcovich, N. E.; Capadona, J. R.; Rowan, S. J.; Weder, C.; Thielemans, W.; Roman, M.; Renneckar, S.; Gindl, W.; Veigel, S.; Keckes, J.; Yano, H.; Abe, K.; Nogi, M.; Nakagaito, A. N.; Mangalam, A.; Simonsen, J.; Benight, A. S.; Bismarck, A.; Berglund, L. A.; Peijs, T. Review: Current International Research into Cellulose Nanofibres and Nanocomposites. *J. Mater. Sci.* **2010**, *45* (1), 1–33. https://doi.org/10.1007/s10853-009-3874-0.

(3) Takahashi, Y.; Ochiai, N.; Matsushita, Y.; Noda, I. Viscoelastic Properties of Poly(2-Vinylpyridine) in Bulk and Solution. *Polym. J.* **1996**, *28* (12), 1065–1070. https://doi.org/10.1295/polymj.28.1065.

(4) Cudjoe, E.; Hunsen, M.; Xue, Z.; Way, A. E.; Barrios, E.; Olson, R. A.; Hore, M. J. A.; Rowan, S. J. Miscanthus Giganteus: A Commercially Viable Sustainable Source of Cellulose Nanocrystals. *Carbohydr. Polym.* **2017**, *155*, 230–241. https://doi.org/10.1016/j.carbpol.2016.08.049.